UC Irvine
UC Irvine Previously Published Works

Title

Conformers of Cysteine and Cysteine Sulfenic Acid and Mechanisms of the Reaction of Cysteine Sulfenic Acid with 5,5-Dimethyl-1,3-cyclohexanedione (Dimedone)

Permalink

https://escholarship.org/uc/item/83k03425

Journal

The Journal of Physical Chemistry B, 117(50)

ISSN

1520-6106

Authors

Freeman, Fillmore
Adesina, Ifeoluwa Taiwo
Le La, Julie
et al.

Publication Date

2013-12-19

DOI

10.1021/jp409022m

Copyright Information

This work is made available under the terms of a Creative Commons Attribution License, available at https://creativecommons.org/licenses/by/4.0/

Peer reviewed

eScholarship.org Powered by the California Digital Library
University of California

THE JOURNAL OF PHYSICAL CHEMISTRY B

Article

pubs.acs.org/JPCB

Conformers of Cysteine and Cysteine Sulfenic Acid and Mechanisms of the Reaction of Cysteine Sulfenic Acid with 5,5-Dimethyl-1,3-cyclohexanedione (Dimedone)

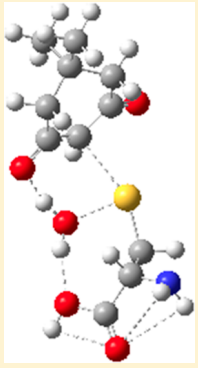
Fillmore Freeman,*[,†] Ifeoluwa Taiwo Adesina,[†] Julie Le La,[†] Joseph Yonghun Lee,[†] and Amelia Ann Poplawski[‡]

[†]Department of Chemistry, University of California, Irvine, Irvine, California 92697, United States

[‡]Department of Chemistry, Misericordia University, Dallas, Pennsylvania 18612, United States

Supporting Information

ABSTRACT: Equilibrium and molecular structures, relative energies of conformers of gaseous cysteine (Cys, C, Cys-SH) and gaseous cysteine sulfenic acid (Cys-SOH), and the mechanisms of the reaction of Cys-SOH with 3-hydroxy-5,5-dimethyl-2-cyclohexen-1-one, the enol tautomer of 5,5-dimethyl-1,3-cyclohexadione (dimedone), have been studied using BD(T), CCSD(T), and QCISD(T) with the cc-pVTZ basis set and using MP2 and the density functionals B3LYP, B3PW91, PBE1PBE, PBEh1PBE, M062X, CAM-B3LYP, and WB97XD with the 6-311+G(d,p) basis set. The structures of the six lowest energy conformers of gaseous Cys-SOH are compared with the six lowest energy conformers of gaseous cysteine (Cys-SH). The relative stability of the six lowest energy conformers of Cys-SH and Cys-SOH are influenced by the interplay among many factors including dispersive effects, electronic effects, electrostatic interactions, hydrogen bonds, inductive effects, and noncovalent interactions. The mechanism of the addition of the lowest energy conformer of cysteine sulfenic acid (Cys-SOH) to dimedone may proceed through a six-membered ring transition state structure and through cyclic hydrogen-bonded transition state structures with one water molecule (8-membered ring), with two water molecules (10-membered ring), and with three water molecules (12-membered ring). Inclusion of one and two water molecules in the transition state structures lowers the activation barrier, whereas inclusion of a third water molecule raises the activation barrier.

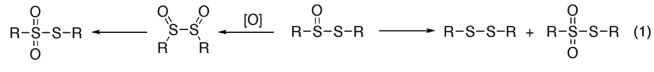


INTRODUCTION

Sulfenic acids are unstable compounds and only a few have been isolated. Owing in part to their high reactivity and instability, relatively little is known about their chemistry, properties, and structural parameters. However, sulfenic acids and their derivatives are useful reagents that play important roles as reactive intermediates in organosulfur chemistry and are implicated in a wide range of biochemical and chemical reactions.[1−45] Sulfenic acids have been trapped with 1,3-dicarbonyl compounds, alkenes, alkynes, and dienes.[19−25] Sulfenic acids are found in biological systems, are transient intermediates in certain protein functions in regulation, play vital roles in catalytic and signaling functions in proteins,[1−4] and are found in natural products including garlic and onion.[37−45]

The semiessential amino acid cysteine [(2*R*)-2-amino-3-sulfhydrylpropanoic acid, Cys, C, Cys-SH, **1**, Chart 1)], which has a structure similar to its precursor serine (Ser, S), is one of two sulfur-containing amino acids isolated from proteins. It is an important functional and structural component of many proteins. The nucleophilic sulfanyl group in (**1**) is sensitive to oxidation−reduction reactions and is easily oxidized by reactive oxygen species (ROS, H_2O_2, ROOR, radicals, nitrogen monoxides, ozone, singlet oxygen) to cysteine sulfenic acid [(2*R*)-2-amino-3-(hydroxysulfanyl)propanoic acid, Cys-SOH, **2**)], which can be oxidized to cysteine sulfinic acid (**3**) and to cysteine sulfonic acid (**4**, Chart 1). Cysteine (**1**) may also be oxidized to the disulfide cystine (**5**, Chart 1). Protein thiols may be oxidized to protein sulfenic acids, disulfides, and to reversible and irreversible intermediates and products. It was shown in the iron-containing nitrile hydratase (NHase), whose active sites were thought to contain three proteinogenic cysteine residues bound to the active catalytic center, that one was a cysteine thiolate, and two of them were post-translationally modified to a cysteine sulfenic acid and to a cysteine sulfinic acid, respectively.[27,32−35] This was the first observation of an iron site with a ligand field containing sulfur in three different oxidation states.

Cysteine sulfenic acid (**2**) can disproportionate to **4** and **5**,[36] as well as undergo cyclodehydration to cysteine (cystine) thiosulfinate (**6**, Chart 1).[5] Thiosulfinates may disproportionate to thiosulfonates (**7**) and disulfides and may be oxidized to unstable vicinal disulfoxides, with relatively weak sulfur−sulfur bonds, that can generate sulfur radicals and/or rearrange to thiosulfonates (**7**, Chart 1, eq 1).[46−50]

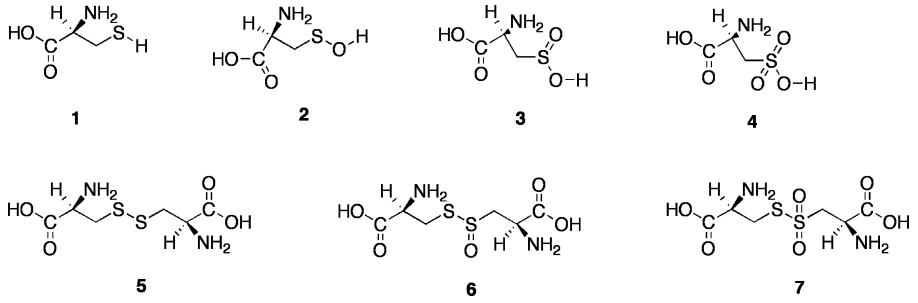


(1)

Received: September 14, 2013
Revised: November 22, 2013
Published: November 25, 2013

 © 2013 American Chemical Society dx.doi.org/10.1021/jp409022m | *J. Phys. Chem. B* 2013, 117, 16000−16012

Chart 1. Organosulfur Compounds Cysteine (1), Cysteine Sulfenic Acid (2), Cysteine Sulfinic Acid (3), Cysteine Sulfonic Acid (4), Cystine (5), Cysteine Thiosulfonate (6), and Cysteine Thiosulfonate (7)



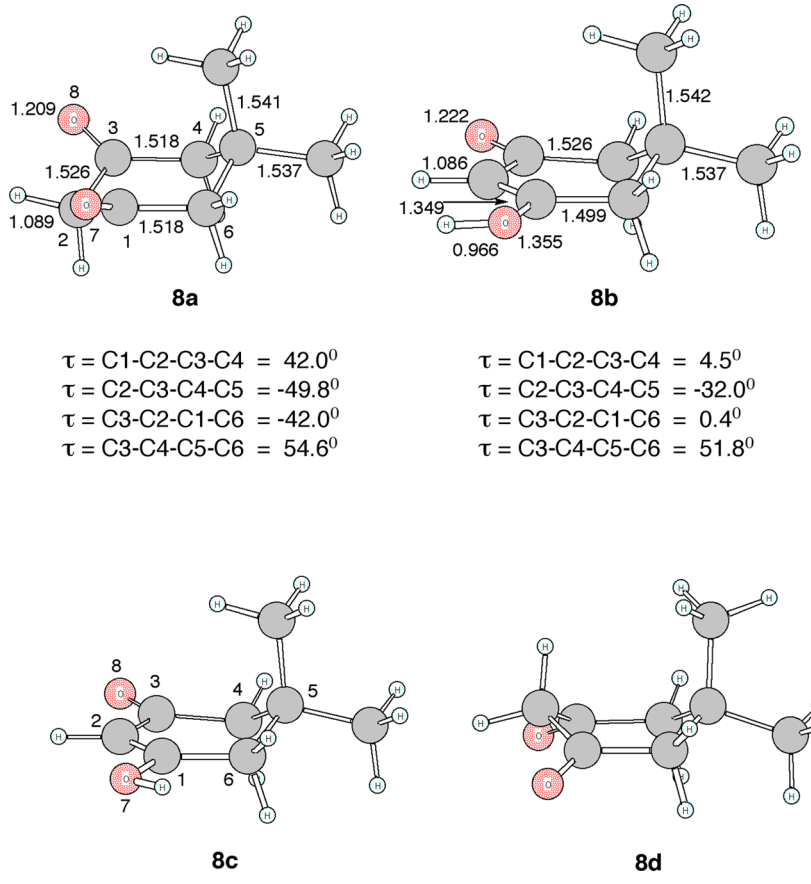
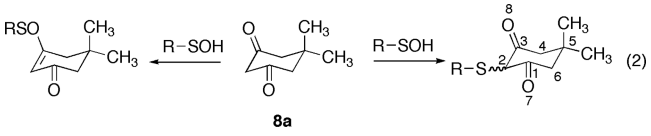


Figure 1. Atom numbering in the B3LYP/6-311+G(d,p) geometry optimized diketo chair (**8a**), *cis*-ketoenol (**8b**), *trans*-ketoenol (**8c**), and diketo boat (**8d**) tautomers of 5,5-dimethyl-1,3-cyclohexanedione (dimedone).

Although reaction mechanisms and structures of sulfenic acids cannot be satisfactorily investigated using traditional experimental methods, considerable information and insight about their structures and chemical and physical properties can be obtained from the results of computational quantum chemistry studies, available experimental studies,[3,4,8,18,51−54] and theoretical chemistry studies. The elusive sulfenic acids have been trapped with 3-hydroxy-5,5-dimethyl-2-cyclohexen-1-one (**8b**), the enol tautomer of dimedone (5,5-dimethyl-1,3-cyclohexadione, **8a**, eq 2),[3,4,55] with 1,3-cyclopentanediones,[56] with 7-chloro-4-nitrobenzo-2-oxa-1,3-diazole (NBD-Cl),[57] and with other probes including biotinylated dimedone analogues for affinity purification, azide "tailed" dimedone for "click" chemistry, and fluorophore-linked dimedone derivatives for visualization. Sulfenic acid modified proteins can be identified by in situ labeling of intact cells or by labeling at the time of lysis using derivatives of dimedone (**8**), 1,3-cyclohexanedione, and 1,3-cyclopentanedione. Evidence for a stabilized cysteine sulfenic acid in a synthetic peptide has been reported.[58] Owing to the importance and significance of the chemoselectivity of dimedone (**8**) and its derivatives in detecting protein sulfenic acids, it is important to understand the mechanisms of their reactions. Although not well studied, sulfenic acids have electrophilic and nucleophilic character and undergo self-condensation reactions[5] and react with alkenes, alkynes, amides, amines, hydrazines, and triphenylphosphine.[3,4,19−25,53] Although the reactions of sulfenic acids with dimedone (**8**) are generally written as resulting in C-sulfenylation at C2, O-sulfenylation to form the sulfenate ester is also possible (eq 2). In addition, a sulfenic acid may also react with the double bond

dx.doi.org/10.1021/jp409022m | J. Phys. Chem. B 2013, 117, 16000−16012

in the enol form (**8b**) of dimedone and other 1,3-dicarbonyl compounds.



8a

COMPUTATIONAL AND THEORETICAL METHODS

Calculations were carried out with the Gaussian[59] and Spartan[60] computational programs. Initial approaches for locating the lowest energy conformers and rotamers included conformational searches at various levels of theory. Several levels of theory were employed in the screening evaluation because at a given level some of the conformers are isoenergetic and the lowest energy conformer from one level of theory does not uniformly translate into the lowest energy conformer at another level. The structures of the lowest energy conformers were confirmed by calculations at several high levels of modern electronic theory.

No constraints were imposed on the structures in the equilibrium geometry calculations or in the transition structure optimizations. Equilibrium geometry and frequency calculations were carried out using the density functionals B3LYP,[61] B3PW91,[62] PBE1PBE,[63] PBEh1PBE,[64] M062X,[65] CAM-B3LYP,[66] and WX97XD,[67] as well as with MP2[68] and the triple-ζ 6-311+G(d,p) basis set.[59,60] Both diffuse and polarization functions are needed for the determination of accurate structures and relative energies of systems containing multiple hydrogen bonds and nonbonding interactions. Single point energy calculations were carried out on geometry optimized structures using coupled cluster theory including the singles doubles with perturbative triples excitations [CCSD(T)],[69,70] the quadratic configuration interaction singles, doubles, and triples method [QCISD(T)],[71] and the Brueckner Doubles Method with triples contributions added [BD(T)][72] in conjunction with the correlation consistent polarized valence cc-pVTZ basis set.[73] The relative energies (E_{rel}) and energy barriers include the electronic energies plus the zero point vibrational energies (ZPVE).

Vibrational frequency analyses were carried out in order to assess the nature of the stationary points and to obtain zero point vibrational energies. The characteristics of local minima and transition states were verified by establishing that the former did not have an imaginary frequency and that the latter had one imaginary frequency. The vibrational frequencies in the text and in the tables were not scaled.[74,75] Intrinsic reaction coordinate (IRC) calculations were used to unambiguously connect transition state structures to their respective reactants and products.[76] The charge distribution was analyzed using natural population analysis (NPA, Natural Bond Order).[77]

Bond angles and dihedral or torsion angles (τ) are given in degrees, bond lengths, and nonbonded distances in angstroms (Å), total energies in atomic units (au), and relative energies in kcal/mol. Atomic charges are given in electrons, dipole moments (μ) in debye (D), infrared intensities in km mol^{-1}, and vibrational frequencies in wave numbers (cm^{-1}).

RESULTS AND DISCUSSION

Although new quantum chemical methods are being developed, it is not an easy task to select the appropriate levels of theory that will give the most accurate results in terms of barrier heights, noncovalent interactions, structural features, transition state properties, and vibrational frequencies. In order to obtain accurate information concerning the optimum levels of theory for consistently predicting electronic structures, noncovalent interactions, and relative energies, we utilized the density functionals B3LYP, B3PW91, PBE1PBE, PBEh1PBE, M062X, CAM-B3LYP, and WB97XD with the 6-311+G(d,p) basis set and MP2 with the 6-311+G(d,p) basis set. It has been demonstrated that hybrid density functionals combine accuracy with computational speed and ease of use to give reliable predictions and calculation results. B3LYP is the most widely used density functional, M062X is known for predicting accurate activation barriers, CAM-B3LYP is the long-range corrected version of B3LYP using the Coulomb attenuating method, and WB97XD includes empirical dispersion and long-range corrections. CAM-B3LYP and WB97XD will be useful since intramolecular hydrogen bonding and nonbonding interactions influence the biological functions, interactions, and shapes of amino acids, enzymes, peptides, and proteins. BD(T),[72] CCSD(T),[69,70] and QCISD(T)[71] with the cc-pVTZ basis set[73] were used for high level energy calculations. CCSD(T) is known to give excellent energy results and, as will be seen below, BD(T) and QCISD(T) predict very similar or the same relative energy values as CCSD(T).

Table 1. Relative Energies of Tautomers of Dimedone (8)

	E_{rel}[a]	
level of theory	*cis*-**8b**	*trans*-**8c**
B3LYP[b]	2.9	4.8
B3PW91[b]	2.7	4.7
B3P86[b]	2.3	4.3
PBE1PBE[b]	2.7	4.7
PBEh1PBE[b]	2.7	4.7
HSEh1PBE[b]	2.6	4.6
O3LY[b]	3.4	5.3
M062X[b]	3.3	5.3
B97D[b]	4.2	5.9
CAM-B3LYP[b]	3.5	5.6
WB97XD[b]	4.7	6.7
BD(T)[c,d]	3.1	5.0
CCSD(T)[c,d]	3.2	5.1
QCISD(T)[c,d]	3.3	5.2

[a] $E_{rel} = E_{ketoenol\ tautomer} - E_{diketo\ tautomer\ (8a)}$. [b] 6-311+G(d,p) basis set. [c] cc-pVTZ basis set. [d] B3LYP/6-311+G(d,p) optimized structure.

Electronic and Molecular Structures. Dimedone (**8**) can exist in the diketo chair form (**8a**, C_s, μ = 4.1) and in the ketoenol half-chair forms (*cis*-**8b**, C2−H and H−O7 are cis, μ = 3.6) and (*trans*-**8c**, C2−H and H−O7 are trans, μ = 5.9, eq 2, Figure 1).[78−84] Although 1,3-cyclohexanedione has a boat diketo form, the boat diketo structure (**8d**) of dimedone optimizes to the diketo chair tautomer (**8a**). Rotamers **8b** and **8c** can be interconverted by rotation about the C1−O7 bond and the computed C1−C2−C3 bond angles in **8a**, **8b**, and **8c** are 113.4°, 121.4°, 121.3°, respectively. The DFT methods predict half-chair conformations for the ketoenol tautomers **8b** and **8c**, which resemble the half-chair conformation of cyclohexene (eq 2, Figure 1). In the B3LYP/6-311+G(d,p) geometry optimized half-chair conformation of cyclohexene the C1−C2=C3−C4 and C1−C6−C5−C4 dihedral angles are 1.6° and 60.2°, respectively, which are similar to those in **8b** and **8c** (Figure 1). The ketoenol form (**8b**) may also exist as dimeric and polymeric structures as solids and in solution.[80−82] The enol crystal structure of dimedone (**8b**) has been described as having an envelope conformation with C1, C2, C3, C4, and

dx.doi.org/10.1021/jp409022m | J. Phys. Chem. B 2013, 117, 16000−16012

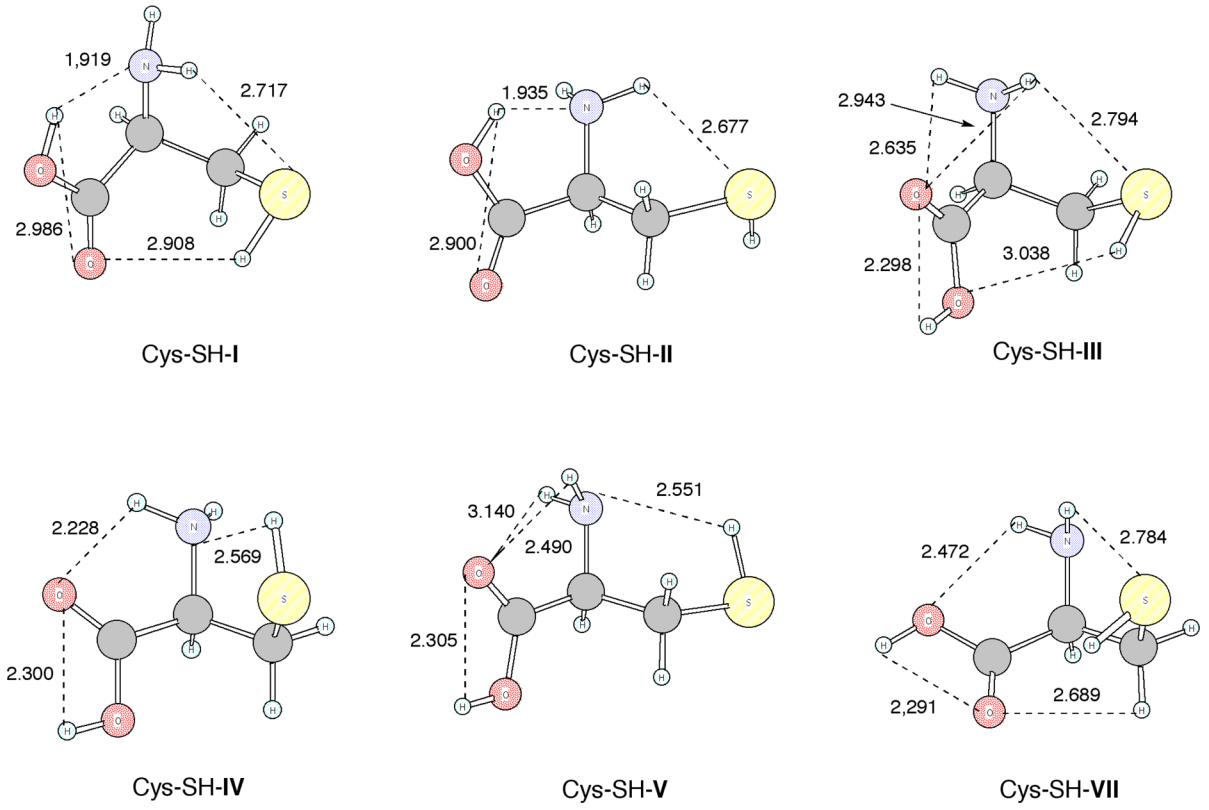


Figure 2. Noncovalent distances in the B3LYP/6-311+G(d,p) geometry optimized lowest energy conformers of cysteine (Cys-SH).

C6 in a common plane, with C5 above it.[80−82] Table 1 shows that the diketo form (**8a**) is more stable than either the *cis*-ketoenol form (**8b**) or the *trans*-ketoenol form (**8c**, Figure 1). The NPA charges on atoms O7, C1, C2, C3, and O8 in **8a** are −0.539, 0.589, −0.568, 0.589, and −0.539, respectively, and in **8c** they are −0.659, 0.405, −0.382, 0.529, and −0.574, respectively.

It is known that amino acids exist as zwitterions in aqueous solution and in the crystalline state and as conformationally flexible neutral (nonionized) forms in the gas phase. Although the structure and relative energies of conformers of neutral cysteine (**1**, Figure 2) have been extensively studied and discussed,[85−96] there does not appear to be any reports on the structures of the conformers of cysteine sulfenic acid (Cys-SOH, **2**). Obtaining the correct order of relative conformational energies for **1** and **2** is difficult with so many conformers within such a small energy range. However it is seen in Table 2 that the results in this study and the results from previous high-level computational quantum chemistry studies in the chemical literature[85−88,90] predict conformer Cys-SH-**I** to be the lowest energy structure for cysteine (**1**, Figure 2). Conformer Cys-SH-**I** is stabilized by intramolecular hydrogen bonds (O−H···N, S−H···O═C, N−H···S), dispersive and steric interactions, and electrostatic, exchange, and hyperconjugative electronic effects.[87]

Structural differences and similarities among the six lowest energy conformers of gaseous cysteine (**1**, Figure 2) and the six lowest energy conformers of gaseous cysteine sulfenic acid (Cys-SOH, Figure 3) are seen in a comparison of their respective geometry optimized structures. Among the six lowest energy structures of Cys-SOH, all levels of theory used predict structure Cys-SOH-**2** to be the lowest energy conformer (Table 3). A conformation with a *s-cis* carboxyl group (O−H bond is cis relative to the O═C bond) is sometimes lower in energy than its *s-trans* conformation. Interestingly, conformers

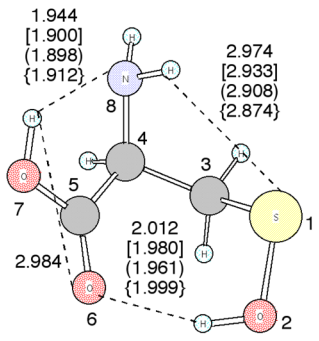
Table 2. Relative Energies of Low Energy Conformers of Cysteine (Cys-SH, I−V, VII)

	E_{rel}[a]					
level of theory	I	II	III	IV	V	VII
BD(T)[b,c]	0.0	1.4	1.8	2.1	1.7	2.1
CCSD(T)[b,c]	0.0	1.4	1.8	2.1	1.7	2.1
QCISD(T)[b,c]	0.0	1.4	1.8	2.1	1.7	2.1
G3[d]	0.0	1.1	1.3	1.5	1.5	2.0
G3[e]	0.0	1.2	1.4	1.7	1.7	2.0
CCSD(T)/CBS[f]	0.0	1.5	1.6	2.0	1.8	2.0
MP2[g]	0.0	1.6	1.8	2.1	2.2	2.2
CCSD[h]	0.0	1.4	1.1	1.6	1.3	1.5
B3LYP[i]	0.0	0.9	1.7	2.1	1.3	1.5
MP2[j]	0.0	1.5	1.3	1.4	1.6	2.1

[a] $E_{rel} = E_{conformer} - E_{conformer\ I}$ in kcal/mol. [b] cc-pVTZ basis set, this study. [c] Computed at the B3LYP/6-311+G(d,p) optimized geometries. [d] G3(MP2)//B3LYP, ref 88. [e] G3, ref 88. [f] Extrapolated from the focal point analysis. Computed at the MP2/aug-cc-pV(T+d)Z reference geometries, ref 87. [g] MP2/aug-cc-pV(T+d)Z Computed at the MP2/aug-cc-pV(T+d)Z reference geometries, ref 87. [h] CCSD/aug-cc-pV(T+d)Z. Computed at the MP2/aug-cc-pV(T+d)Z reference geometries, ref 87. [i] B3LYP/aug-cc-pVTZ. Computed at the B3LYP/aug-cc-pV(T+d)Z reference geometries, ref 87. [j] MP2/aug-cc-pVTZ B3LYP plus zero point energy corrections taken from refs 87, 85, 86, and 90.

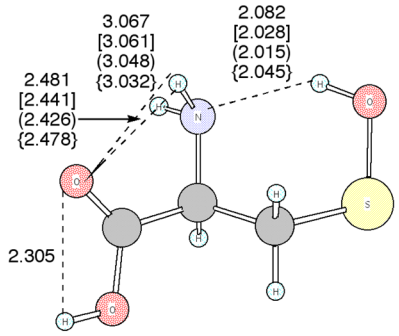
Cys-SH-**I** and Cys-SH-**II**, with *s-trans* carboxyl groups, are lower in energy than the other conformers with *s-cis* carboxyl groups (Figure 2). In contrast, conformer Cys-SOH-**2**, which is structurally similar to Cys-SH-**V** and has a *s-cis* carboxyl group, is lower in energy than conformers Cys-SOH-**1** and Cys-SOH-**5** with *s-trans* carboxyl groups. One conformer may be stabilized more than another, depending on the number and types of intramolecular interactions it has. As in Cys-SH-**I**, Cys-SOH-**2**

dx.doi.org/10.1021/jp409022m | J. Phys. Chem. B 2013, 117, 16000−16012



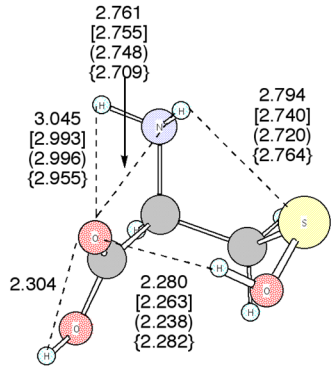
1

τ = H-O2-S1-C3 = -64.3^0
τ = S1-O2-H-O6 = 43.3^0
τ = S1-C3-C4-C5 = -55.7^0
τ = S1-C3-C4-N8 = 69.6^0
τ = C3-C4-C5-O6 = -26.7^0
τ = O2-S1-C3-C4 = 97.6^0
τ = O6-C5-C4-N8 = -156.2^0
τ = O7-C5-C4-N8 = 26.2^0



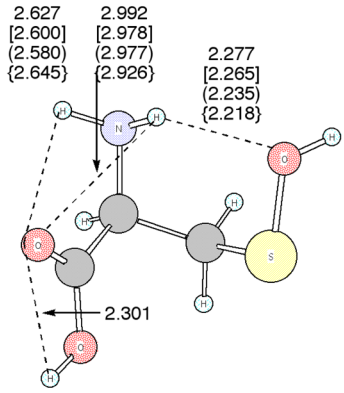
2

τ = H-O2-S1-C3 = -60.8^0
τ = S1-C3-C4-C5 = 176.9^0
τ = S1-C3-C4-N8 = -58.4^0
τ = C3-C4-C5-O6 = 107.5^0
τ = O2-S1-C3-C4 = 73.9^0
τ = O6-C5-C4-N8 = -16.2^0
τ = O7-C5-C4-N8 = 165.1^0



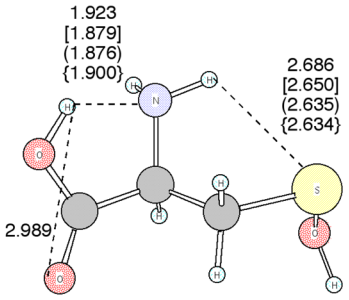
3

τ = H-O2-S1-C3 = -87.2^0
τ = S1-O2-H-O6 = 68.4^0
τ = S1-C3-C4-C5 = -68.9^0
τ = S1-C3-C4-N8 = 57.8^0
τ = C3-C4-C5-O6 = 91.9^0
τ = O2-S1-C3-C4 = 78.4^0
τ = O6-C5-C4-N8 = -32.5^0
τ = O7-C5-C4-N8 = 148.2^0



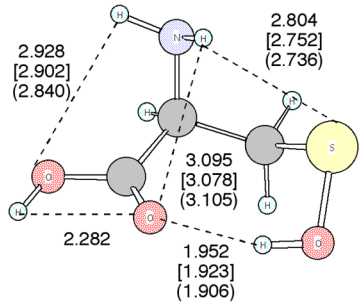
4

τ = H-O2-S1-C3 = -91.3^0
τ = S1-C3-C4-C5 = -55.1^0
τ = S1-C3-C4-N8 = 74.0^0
τ = C3-C4-C5-O6 = 133.2^0
τ = O2-S1-C3-C4 = -67.1^0
τ = O6-C5-C4-N8 = 5.7^0
τ = O7-C5-C4-N8 = -177.4^0



5

τ = H-O2-S1-C3 = -91.6^0
τ = S1-C3-C4-C5 = 178.1^0
τ = S1-C3-C4-N8 = -61.4^0
τ = C3-C4-C5-O6 = -70.9^0
τ = O2-S1-C3-C4 = -57.5^0
τ = O6-C5-C4-N8 = 167.5^0
τ = O7-C5-C4-N8 = -14.3^0



6

τ = H-O2-S1-C3 = -70.4^0
τ = S1-O2-H-O6 = 49.9^0
τ = S1-C3-C4-C5 = -68.3^0
τ = S1-C3-C4-N8 = 56.6^0
τ = C3-C4-C5-O6 = 37.3^0
τ = O2-S1-C3-C4 = 89.8^0
τ = O6-C5-C4-N8 = -87.4^0
τ = O7-C5-C4-N8 = 88.6^0

Figure 3. Atom numbering, torsion angles (τ), and noncovalent distances (B3LYP, [B3PW91], (PBE1PBE), {MP}) in the B3LYP/6-311+G(d,p) geometry optimized lowest energy conformers of cysteine sulfenic acid (Cys-SOH).

is also stabilized by intramolecular interactions owing in part to the polar functional groups (carbonyl C═O, amino NH_2, hydroxyl OH, sulfenic acid SOH), which possess acceptor and donor properties. Cys-SOH-**2** has four strong hydrogen bonding interactions. The carbonyl oxygen atom (O6) in Cys-SOH-**2** forms a bifurcated hydrogen bond with the amino group (4.3 kcal/mol) and there is strong hydrogen bonding between O2−H and N8 (8.6 kcal/mol), as well as between O7−H and O6 (4.3 kcal/mol).[87] Thus, as in Cys-SH-**I**, Cys-SOH-**2** is stabilized by intramolecular hydrogen bonds, dispersive and steric interactions, and electrostatic, exchange, and hyperconjugative electronic effects.

Water Complexes. Water complexes of amino acids play very important roles in biochemistry and biology. The functional groups in Cys-SOH-**2** are capable of participating in

dx.doi.org/10.1021/jp409022m | J. Phys. Chem. B 2013, 117, 16000−16012

Table 3. Relative Energies of Conformers of Cysteine Sulfenic Acid (Cys-SOH-1−Cys-SOH-6)

	E_{rel} [a]					
level of theory	1	2	3	4	5	6
B3LYP[b]	1.7	0.0	1.3	1.0	1.5	1.8
O3LYP[b]	2.0	0.0	1.2	1.5	0.8	1.2
B3PW91[b]	1.2	0.0	1.5	0.9	1.0	2.0
HSEh1PBE[b]	1.0	0.0	1.4	0.6	1.2	1.9
TPSSTPSS[b]	1.0	0.0	1.7	1.0	0.7	1.8
M062X[b]	1.1	0.0	0.5	2.1	2.4	1.6
MP2[b]	2.1	0.0	1.0	0.2	1.9	[e]
B97D[b]	1.3	0.0	0.9	1.3	1.3	1.9
CAM-B3LYP[b]	1.5	0.0	1.4	2.5	1.8	1.8
WB97XD[b]	1.3	0.0	1.0	2.5	1.7	1.9
BD(T)[c,d]	0.9	0.0	1.3	0.5	1.6	1.9
CCSD(T)[c,d]	0.9	0.0	1.3	0.5	1.6	1.9
QCISD(T)[c,d]	0.8	0.0	1.3	0.5	1.6	1.9

[a] $E_{rel} = E_{conformer} - E_{conformer\ 2}$. [b] 6-311+G(d,p) basis set. [c] cc-pVTZ basis set. [d] B3LYP/6-311+G(d,p) optimized structure. [e] Conformer **6** optimized to conformer **3**.

nonbonding interactions and hydrogen bonding that leads to a large number of possible Cys-SOH-**2** water complexes of varying relative stabilities. One example is adding water molecules to both the amino and sulfenic acid groups (Figure 4) and another example is adding water molecules to the carboxyl group (Figure 5). It is seen that the sulfenic acid functional group and the strong intramolecular nonbonding and hydrogen bonding interactions involving the amino group strongly influence the conformational structure of Cys-SOH-**2**. The search for low energy Cys-SOH-**2** water complexes for this study included the objective to have the amino and sulfenic acid groups of the reactant complexes to maintain the same structure as the water free Cys-SOH-**2** structure (Figure 4).

Infrared Spectroscopy. The frequencies and line intensities in the infrared (IR) absorption spectrum are unique identifiers for the structure and provide information on the forces that hold the molecule together. Thus, computed vibrational spectra of molecules in the gas phase are valuable in conformational and structural studies. In addition, accurate computations of vibrational spectra are important in the interpretation of experimental results and experimental spectra. It has been shown that B3LYP with diffuse basis set, which was used in this study, offers a cost-effective choice for predicting molecular vibrational properties.[74,75] The infrared spectra of aliphatic amino acids are generally reported as hydrochlorides or other salts, as sodium or other cation salts, or as zwitterions. A recent infrared photodissociation (IRPD) spectral study of a proline-chloride anion cluster indicated that proline is in its neutral form as opposed to a zwitterion.[97]

Table 4 summarizes the calculated characteristic and informative frequencies of the six lowest energy gaseous conformers

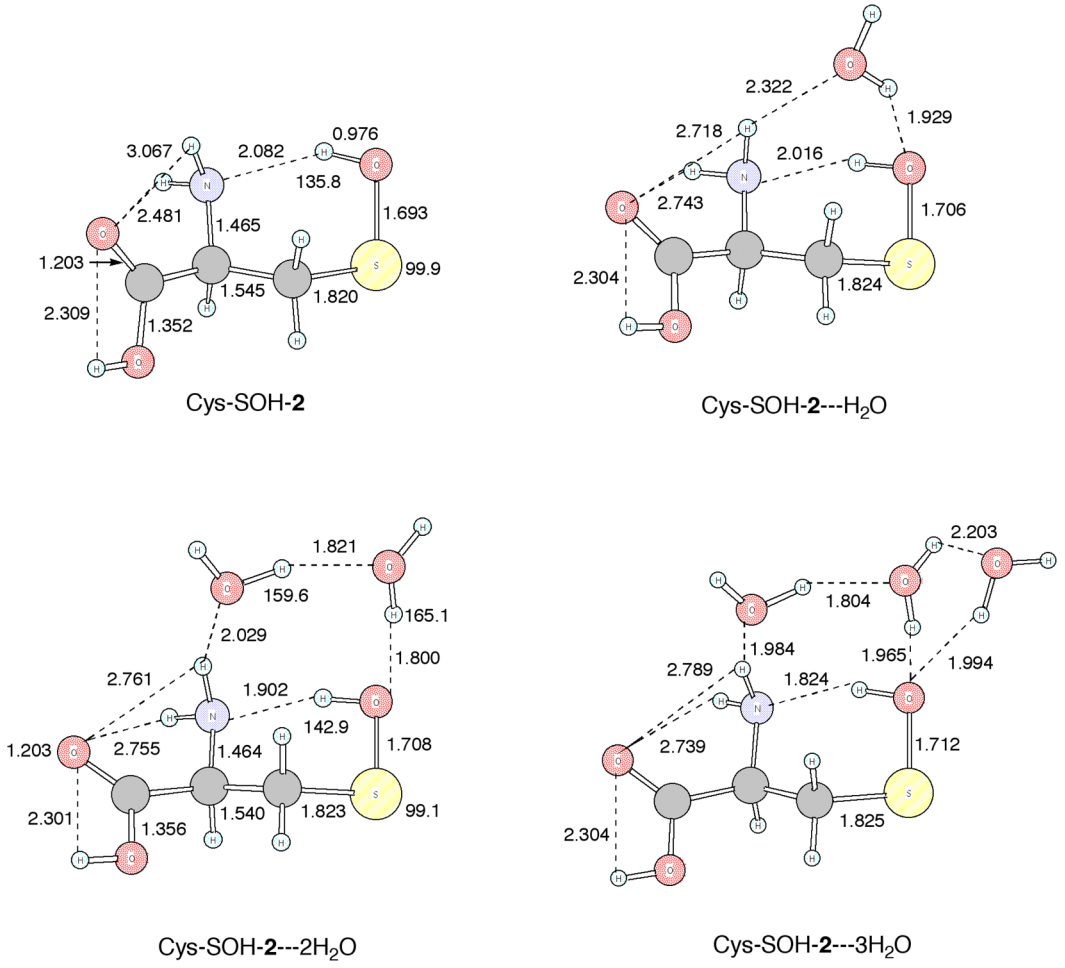


Figure 4. Hydrogen bonds and examples of the B3LYP/6-311+G(d,p) geometry optimized structures of cysteine sulfenic acid (Cys-SOH-2) one-, two-, and three-water complexes involving the amino and sulfenic acid groups.

dx.doi.org/10.1021/jp409022m | J. Phys. Chem. B 2013, 117, 16000−16012

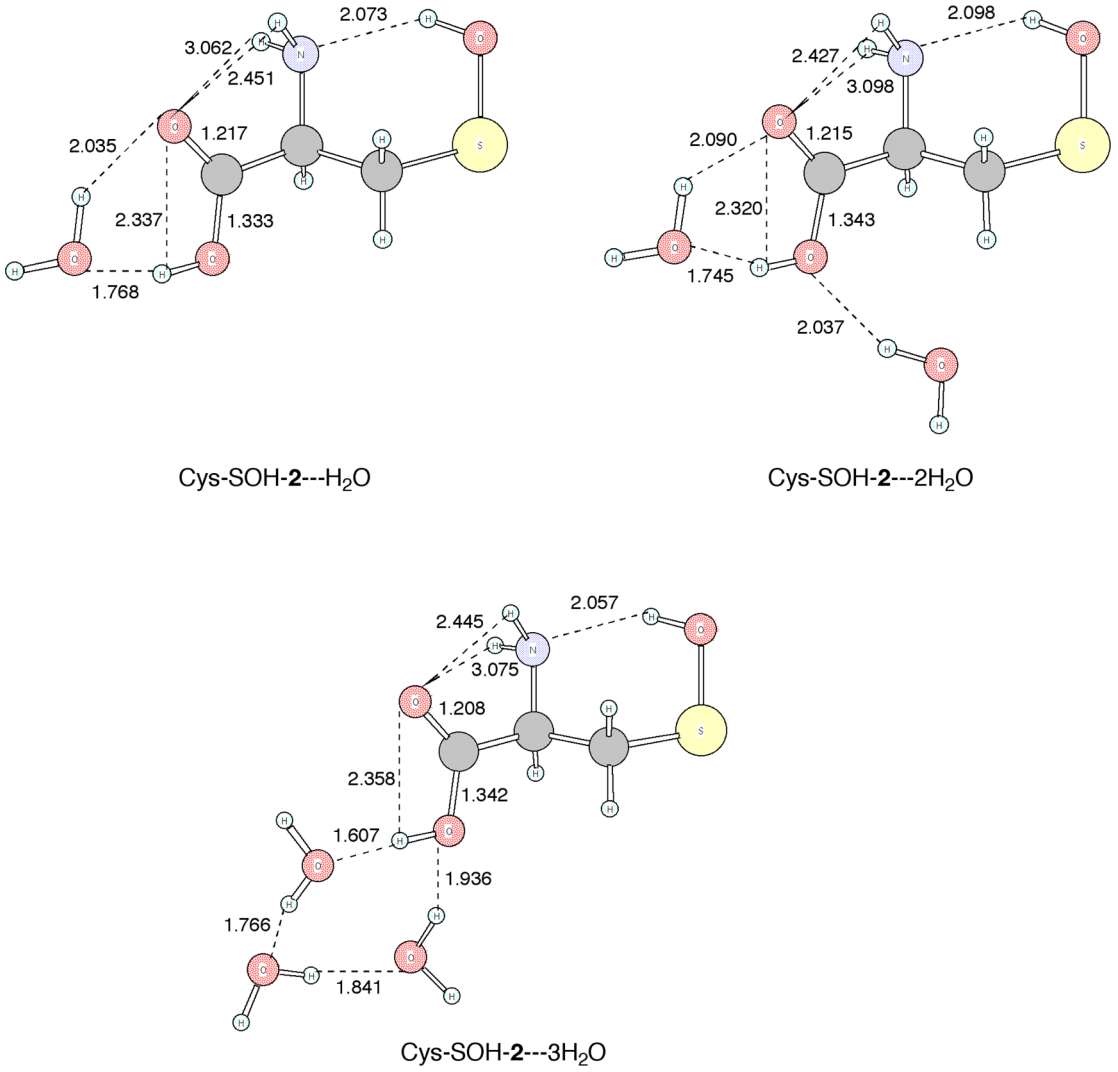


Figure 5. Hydrogen bonds and examples of the B3LYP/6-311+G(d,p) geometry optimized structures of cysteine sulfenic acid (Cys-SOH) one-, two-, and three-water complexes involving the carboxyl group.

Table 4. Calculated Characteristic Infrared Stretching Vibrations and Intensities of Conformers (Cys-SOH-1−Cys-SOH-6) of Cysteine Sulfenic Acid

bond[a,b]	1	2	3	4	5	6
S−C	660 (12)	649 (4)	682 (6)	657 (16)	654(8)	637 (21)
S−O	733 (40)	730 (24)	725 (61)	712 (53)	722 (70)	735 (35)
C−O[c]	1208 (29)	1118 (117)	1174 (58)	1143 (31)	1202 (22)	1156 (41)
C═O	1813 (289)	1809 (324)	1792 (262)	1819 (303)	1834 (359)	1783 (288)
O7−H	3503 (197)	3749 (77)	3743 (77)	3754 (68)	3470 (248)	3741 (67)
N−H sym	3482 (42)	3487 (10)	3504 (4)	3501 (12)	3496 (18)	3496 (5)
N−H asym	3584 (12)	3565 (14)	3584 (11)	3579 (20)	3566 (24)	3590 (13)
O2−H	3665 (170)	3596 (218)	3755 (885)	3790 (77)	3786 (82)	3676 (227)

[a]B3LYP/6-311+G(d,p) optimized structure. [b]Relative intensities are in parentheses. [c]Other C−O vibrations as well as C−N vibrations also occur in this region.

(Cys-SOH-**1**−Cys-SOH-**6**) of cysteine sulfenic acid, which are similar to those calculated and observed for cysteine (Cys-SH, **1**).[85−87,90,92] The relatively weak C−S stretching bands for the conformers of cysteine sulfenic acid (Cys-SOH-**1**−Cys-SOH-**6**) are observed in the 660 ± 23 cm^{-1} region and the O−S stretching vibrations are observed in the 724 ± 13 cm^{-1} region. The C−O stretch region is between 1118 and 1208 cm^{-1} and the strong C═O stretching vibrations range is from 1783 to 1834 cm^{-1}. The N−H asymmetric stretching vibrations give rise to strong bands in the 3578 ± 13 cm^{-1} region and the weaker symmetric N−H stretching bands appear in the 3493 ± 11 cm^{-1} region. The strong O2−H stretching bands of the sulfenic acid groups are in the 3728 ± 63 cm^{-1} region and the strong O7−H stretching vibrations of the carboxyl groups are in the 3612 ± 142 cm^{-1} region. It is also seen in Table 4 that the intensities of the O2−H stretching vibrations of the sulfenic

dx.doi.org/10.1021/jp409022m | J. Phys. Chem. B 2013, 117, 16000−16012

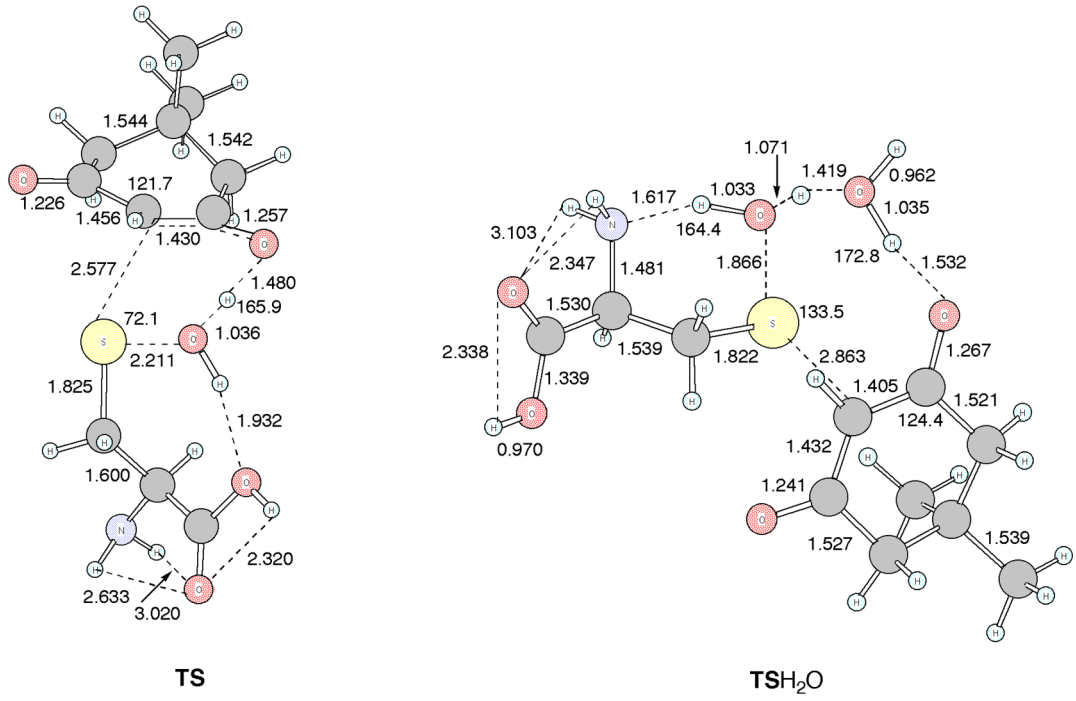


Figure 6. B3LYP/6-311+G(d,p) optimized zero water (**TS**) and one water-assisted (TSH_2O) transition state structures for the reaction of cysteine sulfenic acid (Cys-SOH-**2**) with the ketoenol (**8b**) tautomer of 5,5-dimethyl-1,3-cyclohexanedione (dimedone).

Table 5. Energy Barriers to the Addition of Cysteine Sulfenic Acid (Cys-SOH-2) to Ketoenol (8b) Through Zero Water (TS) and Water-Assisted (TSH_2O, $TS2H_2O$, $TS3H_2O$) Transition States

	ΔE^a			
level of theory	TS_{gas}	TSH_2O	$TS2H_2O$	$TS3H_2O$
B3LYP[b]	40.4	18.2	14.2	25.9
B3PW91[b]	41.3	17.3	11.6	23.8
PBE1PBE[b]	40.2	20.1	8.4	18.0
PBEh1PBE[b]	39.9	21.2	8.2	17.7
M062X[b]	42.2	22.1	8.7	19.2
CAM-B3LYP[b]	45.4	18.0	15.0	27.4
WB97XD[b]	51.1	17.0	11.9	23.2

[a] $\Delta E = E_{transition\ state} - E_{reactants}$. [b] 6-311+G(d,p) basis set.

Table 6. NPA Charges for Cys-SOH-2, CySOH Water Complex ($2\cdots H_2O$), Ketoenol (8b), Transition States TS and TSH_2O, and Water

atom[a]	H_2O	TS	$2\cdots H_2O$	TSH_2O
H_a	0.458		0.487	0.526
O1	−0.916		−0.966	−0.970
H_b	0.458		0.465	0.484
		8b		
	gas	**TS**		TSH_2O
C1	0.425	0.514		0.505
O7	−0.664	−0.667		−0.736
O7−H	0.477	0.501		0.523
C2	−0.416	−0.416		−0.488
C3	0.532	0.502		0.495
O8	−0.576	−0.562		−0.665
		Cys-SOH-**2**		
	gas	**TS**	$2\cdots H_2O$	TSH_2O
S1	0.472	0.370	0.470	0.485
O2	−0.836	−0.862	−0.867	−0.832
O2−H	0.496	0.500	0.506	0.514
C3	−0.549	−0.565	−0.554	−0.574
C4	−0.140	−0.147	−0.134	−0.130
C5	0.794	0.801	0.793	0.796
O6	−0.599	−0.579	−0.594	−0.601
O7	−0.689	−0.734	−0.696	−0.667
O7−H	0.496	0.496	0.489	0.495
N8	−0.863	−0.828	−0.874	−0.859
N8−H_a	0.377	0.364	0.396	0.398
N8−H_b	0.369	0.363	0.373	0.385

[a] B3LYP/6-311+G(d,p) optimized structures.

acid groups are stronger than those of the O7−H carboxylic acid stretching vibrations.

Reaction Mechanism. The sulfur atom in a sulfenic acid has an oxidation state of zero and the presence of the electronegative oxygen lowers the electron density and increases the electrophilicity of the sulfenyl sulfur. The electrophilic sulfenyl sulfur can react with nucleophiles such as alkenes, enamines, and enols. It is reasonable to expect sulfenic acids to undergo electrophilic addition reactions with the ketoenol tautomer (**8b**) of dimedone to form thioethers (sulfides, sulfenylation, eq 2). Thus, in the gas phase, Cys-SOH-**2** will react exothermically with ketoenol (**8b**) through a distorted cyclic six-membered transition state structure (**TS**, Figure 6) to afford the thioether product (eq 2). The flow of electrons, bond breaking, and bond making during the reaction of Cys-SOH-**2** and ketoenol (**8b**) are shown in the transition state structure **TS** (Figure 6). The O7···H···O distances of 1.480 and 1.036 suggest that the proton has been transferred from the ketoenol (**8b**) to the hydroxyl group of the sulfenic acid group in order to convert OH into a better leaving group. Concurrently, the C1−O7 bond is becoming shorter as the carbonyl group is forming, the C1−C2 bond becomes longer as the hybridization

dx.doi.org/10.1021/jp409022m | J. Phys. Chem. B 2013, 117, 16000−16012

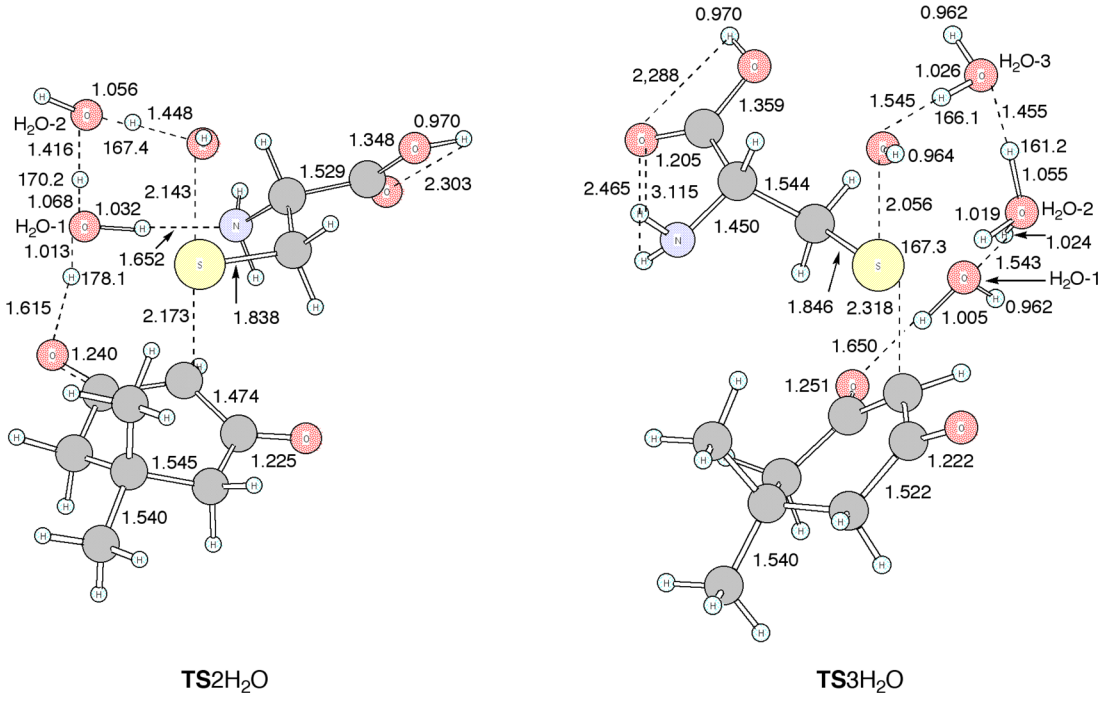


Figure 7. B3LYP/6-311+G(d,p) optimized two water and three water-assisted transition state structures for the reaction of cysteine sulfenic acid (Cys-SOH-**2**) with the ketoenol tautomer of 5,5-dimethyl-1,3-cyclohexanedione (dimedone).

at the carbons is changing from sp^2 to sp^3, and C2−S bond formation is occurring. In addition, there is hydrogen bonding in transition state **TS** between the hydrogen of the OH of the sulfenic acid and O7 of the carboxylic acid. The C2−S−O angle in transition state structure **TS** is 72.1° and the C1−C2−C3 bond angle of ketoenol (**8b**) and its half-chair conformation do not change in going from the ground state to transition state structure **TS** (dihedral angle = C3−C2−C1−C6 = 2.6° and C3−C4−C5−C6 = 54.3°). The reactants and product were connected by an intrinsic reaction coordinate (IRC) calculation in which the imaginary mode for the transition state is followed in both the forward and reverse directions.[76] Table 5 shows that B3LYP, B3PW91, PBE1PBE, PBEh1PBE, and M062X predict the activation barrier for the addition of Cys-SOH-**2** to ketoenol (**8b**) through water-free transition state **TS** in the gas phase to be in the range of 39.9 to 42.2 kcal/mol and that CAM-B3LYP and WB97XD predict a larger barrier.

It is seen in Table 5 that inclusion of one water molecule to give the cyclic eight-membered transition state structure **TS**H_2O for the reaction of Cys-SOH-**2** with ketoenol (**8b**) significantly lowers the activation barrier (Figure 6). The seven levels of theory predict an activation barrier in the range of 17.0 to 22.1 kcal/mol, which is lower than that for the reaction path through the water-free transition state **TS**. The addition of water helps to relieve strain in **TS**, stabilize charges, and facilitate the proton transfer from ketoenol (**8b**). The O7−H hydrogen in ketoenol (**8b**) has been transferred farther (1.532) in the water-assisted **TS**H_2O than in the water-free transition state **TS** (1.480), which is consistent with the increased negative charges at C1 and O7 in **TS**H_2O (Table 6). The C2−S−O bond angle (133.5°) and the C2−S distance (2.863) in **TS**H_2O are greater than those in the water-free **TS**, but the S−O distance (1.866) is shorter than that in **TS**. The C1—C2 (1.405), C2—C3 (1.432), and C3—O8 (1.241) bond distances in **TS**H_2O are consistent with electron delocalization. It is seen in **TS**H_2O that there is a nonbonded interaction between the hydrogen of the OH group of the sulfenic acid group and the lone pair on nitrogen (Figure 6). Table 6 shows that the charges have increased at the atoms in water in the 1:1 cysteine water

Table 7. NPA Charges for Cys-SOH-2, CySOH Water Complexes (2···2H_2O, 2···3H_2O), Ketoenol (8b), Water, and Transition States TS2H_2O and TS3H_2O

atom[a]	H_2O	2···2H_2O	TS2H_2O	2···3H_2O	TS3H_2O
H_a	0.458	0.460	0.521	0.488	0.523
O1	−0.916	−0.973	−0.879	−0.958	−0.974
H_b	0.458	0.501	0.514	0.464	0.478
H_c		0.502	0.516	0.494	0.502
O2		−0.983	−0.983	−0.969	−0.897
H_d		0.467	0.478	0.488	0.508
H_e				0.503	0.517
O3				−0.987	−0.910
H_f				0.468	0.490
8b					
C1	0.425		0.589		0.521
O7	−0.664		−0.654		−0.709
O7−H	0.477		0.524		0.509
C2	−0.416		−0.545		−0.509
C3	0.532		0.548		0.510
O8	−0.576		−0.606		−0.688
Cys-SOH-**2**					
S1	0.472	0.472	0.314	0.475	0.453
O2	−0.836	−0.888	−1.023	−0.927	−0.952
O2−H	0.496	0.512	0.452	0.517	0.513
C3	−0.549	−0.551	−0.531	−0.547	−0.524
O6	−0.599	−0.594	−0.609	−0.590	−0.608
O7	−0.689	−0.697	−0.680	−0.697	−0.679
N8	−0.863	−0.885	−0.849	−0.885	−0.867
N8−H_a	0.377	0.414	0.387	0.421	0.380
N8−H_b	0.369	0.373	0.379	0.376	0.369

[a]B3LYP/6-311+G(d,p) optimized structures.

dx.doi.org/10.1021/jp409022m | J. Phys. Chem. B 2013, 117, 16000−16012

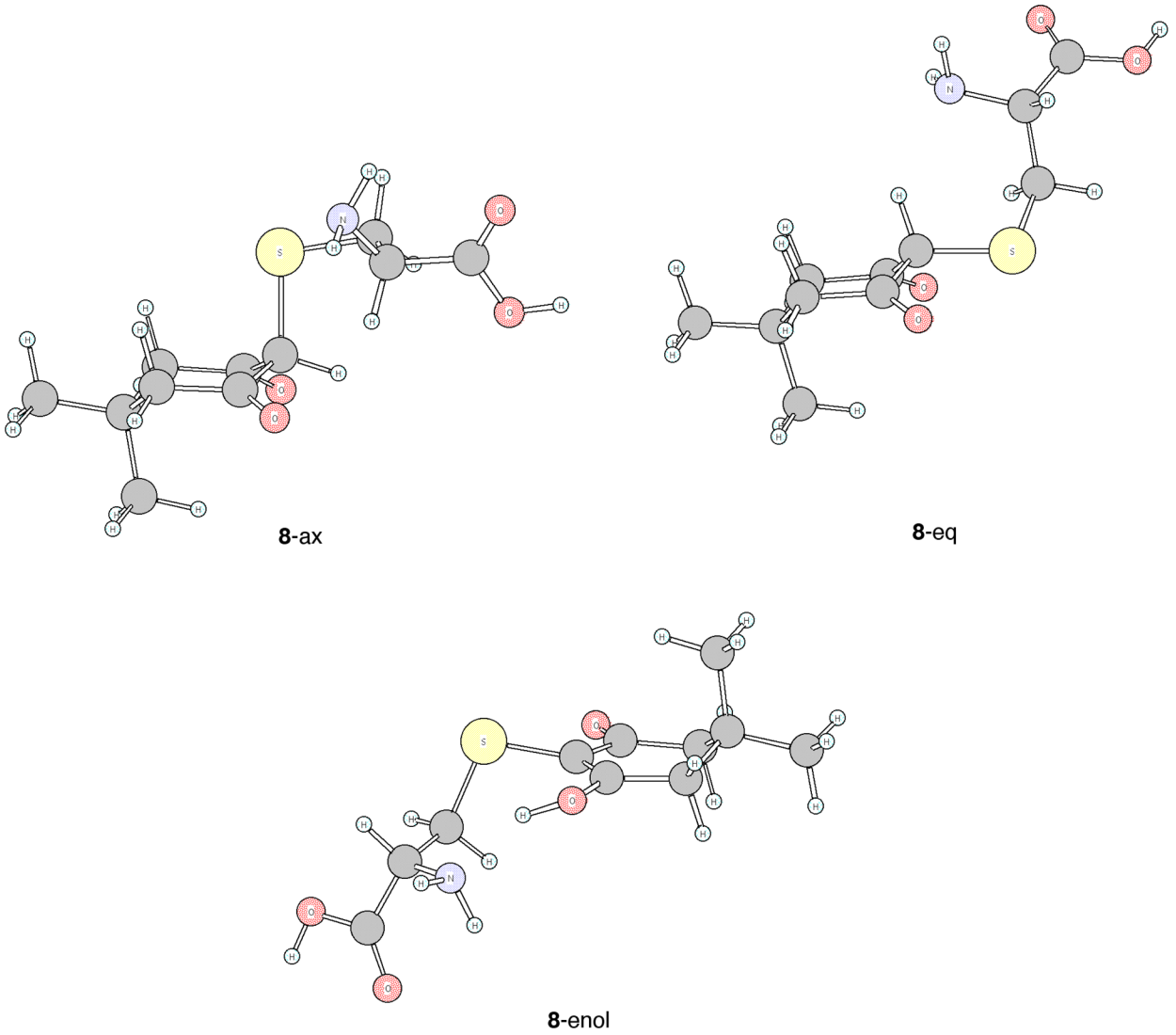


Figure 8. B3LYP/6-311+G(d,p) geometry optimized structures of the enol tautomer (**8**-enol) and the predicted axial (**8**-ax) and equatorial (**8**-eq) thioethers from the reaction of cysteine sulfenic acid (Cys-SOH-**2**) with ketoenol (**8b**).

complex (**2**···H_2O) and in **TS**H_2O. Table 6 shows that the negative charges at C2, O7, and O8 in **8b** have not changed in going to transition state **TS** but are more negative in **TS**H_2O. The positive charge at C3 in **8b** has decreased in going to **TS** and to **TS**H_2O. Relative to **8b**, the positive charge on the sulfur atom is smaller in **TS** and is slightly larger in **TS**H_2O, the charge on the sulfenic acid oxygen (O2) is larger in **TS** and essentially unchanged in **TS**H_2O, and the O2−H has a larger positive charge in **TS**H_2O than in **TS**.

Table 5 also shows that the inclusion of two water molecules to the transition state structure further lowers the activation barrier, but inclusion of a third water molecule raises the activation barrier (Figure 7). The inclusion of water molecules in the transition state structures sets up a system by which the proton from the O7−H bond may diffuse through a hydrogen-bonded network of water molecules in a Grotthuss-type mechanism.[98−102] The O7−H distance in the transition state **TS** is shorter than those in **TS**H_2O, **TS**2H_2O, and **TS**3H_2O, whereas the S−O distance in transition state **TS** is longer than those in **TS**H_2O, **TS**2H_2O, and **TS**3H_2O (Figures 6 and 7). Loss of the proton from ketoenol (**8b**) in the transition state structures leads to more enolate character in **8b** and increased nucleophilicity at C2. The C−S distance in transition state **TS** is shorter than that in **TS**H_2O but is longer than those in **TS**2H_2O and **TS**3H_2O. Although the conformation of the six-membered ring in (**8b**) does not change in going from ground state reactant to the transition state structure **TS** (μ = 4.6), the six-membered rings in **TS**H_2O (μ = 7.0), **TS**2H_2O (μ = 1.8), and **TS**3H_2O (μ = 3.8) have distorted half-chair conformations.

There are larger positive charges on the N−H and O−H hydrogens that are involved in hydrogen bonds than on those that are not involved in hydrogen bonding. In going from ground state to transition state **TS**, the negative charge at C2 in the ketoenol (**8b**) does not change, but it increases in the other three transition states, with the largest increase in **TS**2H_2O (Tables 6 and 7). The negative charge at O7 in the ketoenol (**8b**) is essentially the same in transition state **TS**, decreased in **TS**2H_2O, and increased in **TS**H_2O and **TS**3H_2O, and the positive charges at the O7−H and C1 are increased in the four transition states. The positive charge on C3 in ketoenol (**8b**) increases only in **TS**2H_2O, the negative charge on O7 in **8b** decreases only in transition state **TS**, and the positive charge at sulfur only in transition state **TS**H_2O. The negative charge on

dx.doi.org/10.1021/jp409022m | J. Phys. Chem. B 2013, 117, 16000−16012

O2 is increased in the four transitions states, with the largest change occurring in **TS2H$_2$O**.

The structures of the axial (**8**-ax) and equatorial (**8**-eq) sulfide products from the reaction of the lowest energy conformer (Cys-SOH-**2**) of cysteine sulfenic acid with the ketoenol (**8b**) are shown in Figure 8. The enol isomer (**8**-enol) is 6.5 and 6.4 kcal/mol lower in energy than the respective axial (**8**-ax) and equatorial (**8**-eq) isomers (Figure 8).

The data presented above are consistent with the prediction that the reaction of the lowest energy conformer (Cys-SOH-**2**) of cysteine sulfenic acid with the enol form (**8b**) of dimedone probably proceeds through a ten-membered cyclic hydrogen bonded transition state containing two water molecules (**TS2H$_2$O**, Figure 7). The water molecules assist in orienting the structure of the transition state in order to facilitate the proton transfer process.

CONCLUSIONS

The six lowest energy conformers of the amino acid cysteine (Cys-SH, **1**) were confirmed in the gas phase and the six lowest energy conformers of cysteine sulfenic acid (Cys-SOH, **2**) in the gas phase are reported for the first time. The important structural features and characteristic and informative vibrational frequencies of conformers of Cys-SOH (**2**) are also described. The structures of selected cysteine sulfenic acid 1:1, 1:2, and 1:3 water complexes were also located and investigated. Factors that contribute to the relative stability of conformers of cysteine (Cys-SH, **1**) and cysteine sulfenic acid (Cys-SOH, **2**) in a particular environment include subtle interplay among electronic effects, electrostatic interactions, experimental conditions, inductive effects, intramolecular and intermolecular hydrogen bonding interactions, and steric factors.

Transition state **TS** has the half-chair conformation and transition states **TSH$_2$O**, **TS2H$_2$O**, and **TS3H$_2$O** have distorted half-chair conformations. The mechanism of the reaction of the lowest energy conformer of cysteine sulfenic acid (Cys-SOH-**2**) with 3-hydroxy-5,5-dimethyl-2-cyclohexen-1-one (**8b**), the enol tautomer of 5,5-dimethyl-1,3-cyclohexadione (dimedone, **8**), probably proceeds through a cyclic 10-membered hydrogen-bonded transition state structure with two water molecules (**TS2H$_2$O**) rather than through a water-free 6-membered ring structure (**TS**), or through an 8-membered ring transition state with one water molecule (**TSH$_2$O**), or through a 12-membered ring transition state structure with three water molecules (**TS3H$_2$O**).

ASSOCIATED CONTENT

Supporting Information

The complete citations for refs 59 and 60. This material is available free of charge via the Internet at http://pubs.acs.org.

AUTHOR INFORMATION

Corresponding Author

*Tel.: 949-824-6501. Fax: 949-824-8570. E-mail: ffreeman@uci.edu.

Notes

The authors declare no competing financial interest.

ACKNOWLEDGMENTS

We thank the National Science Foundation for support (NSF CHE-1062891) and for NSF CHE-0840513 that supports the University of California, Irvine Greenplanet computing cluster.

REFERENCES

(1) Conte, M. L.; Carroll, K. S. In *The Chemistry of Thiol Oxidation and Detection in Oxidative Stress and Redox Regulation*; Jakob, U., Reichmann, D., Eds.; Springer: Netherlands, 2013; Chapter 1, pp 1−41.

(2) Poole, L. B.; Nelson, K. J.; Karplus, P. A. In *Sulfenic Acids and Peroxiredoxins in Oxidant Defense and Signaling in Oxidative Stress and Redox Regulation*; Jakob, U., Reichmann, D., Eds.; Springer: Netherlands, 2013; Chapter 4, pp 85−118.

(3) Paulsen, C. E.; Carroll, K. S. Cysteine-Mediated Redox Signaling: Chemistry, Biology, and Tools for Discovery. *Chem. Rev.* **2012**, *113*, 4633−4679 and references therein.

(4) Gupta, V.; Carroll, K. S. Sulfenic Acid Chemistry, Detection and Cellular Lifetime. *Biochim. Biophys.* **2013**, http://dx.doi.org/10.1016/j.bbagen.2013.05.040, and references therein.

(5) Freeman, F.; Bui, A.; Dinh, L.; Hehre, W. J. Dehydrative Cyclocondensation of Hydrogen Thioperoxide and of Alkanesulfenic Acids. *J. Phys. Chem. A* **2012**, *116*, 8031−8039.

(6) Leonard, S. E.; Carroll, K. S. Chemical 'omics' Approaches for Understanding Protein Cysteine Oxidation in Biology. *Curr. Opin. Chem. Biol.* **2011**, *15*, 88−102.

(7) Roos, G.; Messens, J. Protein Sulfenic Acid Formation: From Cellular Damage to Redox Regulation. *Free Radical Biol. Med.* **2011**, *51*, 314−326 and references therein.

(8) Kettenhofen, N. J.; Wood, M. J. Formation, Reactivity, and Detection of Protein Sulfenic Acids. *Chem. Res. Toxicol.* **2010**, *23*, 1633−1646.

(9) Heinecke, J.; Ford, P. C. Formation of Cysteine Sulfenic Acid by Oxygen Atom Transfer from Nitrite. *J. Am. Chem. Soc.* **2010**, *132*, 9240−9243.

(10) McGrath, A. J.; Garrett, G. E.; Valgimigli, L.; Pratt, D. A. *Redox Chem. Sulfenic Acids* **2010**, *132*, 16759−16761.

(11) Lacombe, S.; Loudet, M.; Banchereau, E.; Simon, M.; Pfister-Guillouzo, G. Sulfenic Acids in the Gas Phase: A Photoelectron Study. *J. Am. Chem. Soc.* **1996**, *118*, 1131−1138.

(12) Ortiz, J. V. Electron Propagator Theory of the Photoelectron Spectrum of Methanesulfenic Acid. *J. Phys. Chem. A* **2000**, *104*, 11433−11438.

(13) Patai, S., Ed. *The Chemistry of Sulphenic Acids and their Derivatives*; Wiley-Interscience: New York, 1990.

(14) Wagner, G. Mechanistic Aspects of the Reaction of Dimedone Derivatives with Sulfenic Acids and Other Sulfur Compounds—A Computational Study. *Tetrahedron* **2013**, *69*, 7243−7252.

(15) Rehder, D. S.; Borges, C. R. Cysteine Sulfenic Acid as an Intermediate in Disulfide Bond Formation and Nonenzymatic Protein Folding. *Biochemistry* **2010**, *49*, 7748−7755.

(16) Mansuy, D.; Dansette, P. M. Sulfenic Acids as Reactive Intermediates in Xenobiotic Metabolism. *Arch. Biochem. Biophys.* **2011**, *507*, 174−185.

(17) Drabowicz, J.; Kielbasinski, P.; Lyzwa, P.; Mikolajaczyk, M. Product Class 9: Alkanesulfenic Acids and Acyclic Derivatives. *Sci. Synth.* **2007**, *39*, 543−572.

(18) Aversa, M. C.; Barattucci, A.; Bonaccorsi, P.; Giannetto, P. Recent Advances and Perspectives in the Chemistry of Sulfenic Acids. *Curr. Org. Chem.* **2007**, *11*, 1034−1052.

(19) Menichetti, S.; Aversa, M. C.; Bonaccorsi, P.; Lamanna, G.; Morau, A. Microwave-Assisted Solid-Phase Chemistry for Rapid Efficient Generation and Trapping of Sulfenic Acids. *J. Sulfur Chem.* **2006**, *27*, 393−400.

(20) Aversa, M. C.; Barattucci, A.; Bonaccorsi, P.; Contini, A. Addition of Sulfenic Acids to Monosubstituted Acetylenes: a Theoretical and Experimental Study. *J. Phys. Org. Chem.* **2009**, *22*, 1048−1057.

(21) Benitez, L. V.; Allison, W. S. The Inactivation of the Acyl Phosphatase Activity Catalyzed by the Sulfenic Acid Form of Glyceraldehyde 3-Phosphate Dehydrogenase by Dimedone and Olefins. *J. Biol. Chem.* **1974**, *249*, 6234−6243.

(22) Allison, W. S. Formation and Reactions of Sulfenic Acids in Proteins. *Acc. Chem. Res.* **1976**, *9*, 293−299.

(23) Barrett, A. G. M.; Barton, D. H. R.; Nagubandi, S. Preparation and Trapping of Sulphenic Acids. *J. Chem. Soc., Perkin Trans. 1* **1980**, 237−239.
(24) Jones, D. N.; Hill, D. R.; Lewton, D. A. Synthesis of Sulphoxides by Intramolecular and Intermolecular Addition of Sulphenic Acids to Olefins and Dienes. *J. Chem. Soc., Perkin Trans. 1* **1976**, 1574−1587.
(25) Davis, F. A.; Billmers, R. L. Chemistry of Sulfenic Acids. 6. Structure of Simple Sulfenic Acids Generated by Flash Vacuum Pyrolysis. *J. Org. Chem.* **1985**, *50*, 2593.
(26) Penn, R. C.; Block, E.; Revelle, L. K. Flash Vacuum Pyrolysis Studies. 5. Methanesulfenic Acid. *J. Am. Chem. Soc.* **1978**, *100*, 2622−2623.
(27) Enami, S.; Hoffmann, M. R.; Colussi, A. J. Simultaneous Detection of Cysteine Sulfenate, Sulfinate, and Sulfonate During Cysteine Interfacial Ozonolysis. *J. Phys. Chem. B* **2009**, *113*, 9356−9358.
(28) O'Donnell, J. S.; Schwan, A. L. β-Sulfinyl Acrylate Esters as a Convenient Source of Alkane- and Arenesulfenate Anions. *J. Tetrahedron Lett.* **2003**, *44*, 6293−6296.
(29) O'Donnell, J. S.; Schwan, A. L. Generation, Structure and Reactions of Sulfenic Acid Anions. *J. Sulfur Chem.* **2004**, *25*, 183−211.
(30) Schwan, A. L.; Verdu, M. J.; Singh, S. P.; O'Donnell, J. S.; Ahmadi, A. N. Diastereoselective Alkylations of a Protected Cysteinesulfenate. *J. Org. Chem.* **2009**, *74*, 6851−6854.
(31) Singh, S. P.; O'Donnell, J. S.; Schwan, A. L. Nucleophilic Attack of 2-Sulfinyl Acrylates: A Mild and General Approach to Sulfenic Anions. *Org. Biomol. Chem.* **2010**, *8*, 1712−1717.
(32) Huang, W.; Jia, J.; Cummings, J.; Nelson, M.; Schneider, G.; Lindqvist, Y. Crystal Structure of Nitrile Hydratase Reveals a Novel Centre in a Novel Fold. *Structure* **1997**, *5*, 691−699.
(33) Nagashima, S., Nakasako, M., Dohmae, N., Tsujishima, M., Takio, K., Odaka, M., Yohda, M., Kamiya, N., and Endo, I. Novel Nonheme Iron Center of Nitrile Hydratase with a Claw Setting of Oxygen Atoms. *Nat. Struct. Biol. 5*, 347−351.
(34) Miyanaga, A.; Fushinobu, S.; Ito, K.; Wakagi, T. Crystal Structure of Cobalt-Containing Nitrile Hydratase. *Biochem. Biophys. Res. Commun.* **2001**, *288*, 1169−1174.
(35) Noguchi, T.; Nojiri, M.; Takei, K.; Odaka, M.; Kamiya, N. Protonation Structures of Cys-Sulfinic and Cys-Sulfenic Acids in the Photosensitive Nitriloe Hydratase Revealed by Fourie3r Transform Infrared Spectroscopy. *Biochemistry* **2003**, *42*, 11642−11650.
(36) Yoshimura, T.; Tsukurimichi, E.; Yamazaki, S.; Soga, S.; Shimasaki, C.; Hasegawa, K. Synthesis of a Stable Sulfenic Acid, *trans*-Decalin-9-sulfenic Acid. *J. Chem. Soc., Chem. Commun.* **1992**, 1337−1338.
(37) Block, E. *Garlic and Other Alliums: The Lore and the Science*; Royal Society of Chemistry: Cambridge, U.K., 2010, and references therein.
(38) Amagase, H. Clarifying the Real Bioactive Constituents of Garlic. *J. Nutr.* **2006**, *136*, 716S−725S.
(39) Kubec, R.; Kim, S.; Musah, R. A. S-Substituted Cysteine Derivatives and Thiosulfinate Formation in *Petiveria alliacea*, Part II. *Photochemistry* **2002**, *61*, 675−680.
(40) Vaidya, V.; Ingold, K. U.; Pratt, D. A. Garlic: Source of the Ultimate Antioxidants-Sulfenic Acids. *Angew. Chem., Int. Ed.* **2009**, *48*, 157−160.
(41) Lynett, P. T.; Butts, K.; Vaidya, V.; Garrett, G. E.; Pratt, D. A. The Mechanism of Radical-Trapping Antioxidant Activity of Plant-Derived Thiosulfinates. *Org. Biomol. Chem.* **2011**, *9*, 3320−3330.
(42) Amorati, R.; Lynett, P. T.; Valgimigli, L.; Pratt, D. A. The Reaction of Sulfenic Acids with Peroxyl Radicals: Insights into the Radical-Trapping Antioxidant Activity of Plant-Derived Thiosulfinates. *Chem.—Eur. J.* **2010**, *18*, 6370−6379.
(43) El-Aasr, M.; Fujiwara, Y.; Takeya, M.; Ikeda, T.; Tsukamoto, S.; Ono, M.; Nakano, D.; Okawa, M.; Kinjo, J.; Yoshimitsu, H.; Nohara, T. Onionin A from *Allium cepa* Inhibits Macrophage Activation. *J. Nat. Prod.* **2010**, *73*, 1306−1308.
(44) Freeman, F.; Huang, B.-G.; San, R. I. S. Garlic Chemistry: Nitric Oxide Oxidation of (+)-*S*-(2-Propenyl)-L-Cysteine Sulfoxide. *J. Org. Chem.* **1994**, *59*, 3227−3229.
(45) Freeman, F.; Kodera, Y. Garlic Chemistry: Stability of *S*-(2-Propenyl) 2-Propene-1-sulfinothioate (Allicin) in Blood, Solvents, and Simulated Physiological Fluids. *J. Agric. Food Chem.* **1995**, *43*, 2332−2338.
(46) Freeman, F.; Angeletakis, C. N. α-Disulfoxide and Sulfinic Anhydride in the Peroxy Acid Oxidation of 2-Methyl-2-propyl 2-Methyl-2-propanethiosulfinate. *J. Am. Chem. Soc.* **1981**, *103*, 6232−6235.
(47) Freeman, F. *vic*-Disulfoxides and *O*,*S*-Sulfenyl Sulfinates. *Chem. Rev.* **1984**, *84*, 117−135.
(48) Freeman, F.; Keindl, M. C. Sulfinyl, α-Sulfinyl, Sulfonyl, and α-Sulfonyl Radicals. *Sulfur Rep.* **1985**, *4*, 231−305.
(49) Freeman, F.; Angeletakis, C. N.; Pietro, W. J.; Hehre, W. J. An Ab Initio Molecular Orbital Study of the Rearrangement of α-Disulfoxide to Thiosulfonate. *J. Am. Chem. Soc.* **1982**, *104*, 1161−1165.
(50) Freeman, F.; Angeletakis, C. N. Carbon-13 Nuclear Magnetic Resonance Study of the Conformations of Disulfides and Their Oxide Derivatives. *J. Org. Chem.* **1982**, *47*, 4194−4200.
(51) Rehder, D. S.; Borges, C. R. Possibilities and Pitfalls in Quantifying the Extent of Cysteine Sulfenic Acid Modification of Specific Proteins Within Complex Biofluids. *BMC Biochem.* **2010**, *11*, 25.
(52) Klomsiri, C.; Nelson, K J.; Bechtold, E.; Soito, L.; Johnson, L.; Lowther, W. T.; Ryu, S.-E.; King, S. B.; Furdui, C. M.; Poole, L. B. Use of Dimedone-Based Chemical Probes for Sulfenic Acid Detection: Evaluation of Conditions Affecting Probe Incorporation into Redox-Sensitive Proteins. *Methods Enzymol.* **2010**, *473*, 77−94.
(53) Dalle-Donne, I.; Carini, M.; Orioli, M.; Vistoli, G.; Regazzoni, L.; Colombo, G.; Rossi, R.; Milzani, A.; Aldini, G. Protein Carbonylation: 2,4-Dinitrophenylhydrazine Reacts with Both Aldehydes/Ketones and Sulfenic Acids. *Free Radical Biol. Med.* **2009**, *46*, 1411−1419.
(54) Poole, L. B.; Zeng, B. B; Knaggs, S. A.; Yakuba, M.; King, S. B. Synthesis of Chemical Probes to Map Sulfenic Acid Modifications in Proteins. *Bisconjugate Chem.* **2005**, *16*, 1624−1626.
(55) Seo, Y. H.; Carroll, K. S. Quantification of Protein Sulfenic Acid Modifications Using Isotope-Coded Dimedone and Iododimedone. *Angew. Chem., Int. Ed.* **2011**, *50*, 1342−1345.
(56) Qian, J.; Klomsiri, C.; Wright, M. W.; King, S. B.; Tsang, A. W. Simple Synthesis of 1,3-Cyclopentanedione Derived Probes for Labeling Sulfenic Acid Proteins. *Chem. Commun.* **2011**, *47*, 9203−9205.
(57) Ellis, H. R.; Poole, L. B. Novel Application of 7-Chloro-4-nitrobenzo-2-oxa-1,3-diazol to Identify Cysteine Sulfenic Acid in the AhpC Component of Alkyl Hydroperoxide Reductase. *Biochemistry* **1997**, *36*, 15013−15018.
(58) Shetty, V.; Spellman, D. S.; Neubert, T. A. Characterization by Tandem Mass Spectrometry of Stable Cysteine Sulfenic Acid in a Cysteine Switch Peptide of Matrix Metalloproteinases. *J. Am. Soc. Mass Spectrom.* **2007**, *18*, 1544−1551.
(59) Frisch, M. J.; Trucks, G. W.; Schlegel, H. B.; Scuseria, G. E.; Robb, M. A.; Cheeseman, J. R.; Montgomery, J. A., Jr.; Vreven, T.; Kudin, K. N.; Burant, J. C., et al., *Gaussian 03*, Revision A.1; Gaussian, Inc.: Pittsburgh, PA, 2003.
(60) Kong, J.; White, C. A.; Krylov, A. I.; Sherrill, C. D.; Adamson, R. D.; Furlani, T. R.; Lee, M. S.; Lee, A. M.; Gwaltney, S. R.; Adams, T. R.; et al. *J. Comput. Chem.*; Spartan, Wavefunction, Inc.: Irvine, CA 92612, 2000; Vol. *21*, pp 1532−1548.
(61) Becke, A. D. Density-Functional Thermochemistry. III. The Role of Exact Exchange. *J. Chem. Phys.* **1993**, *98*, 5648−5652.
(62) Burke, K.; Perdew, J. P.; Wang, Y. In *Electronic Density Functional Theory: Recent Progress and New Directions*; Dobson, J. F., Vignale, G., Das, M. P., Eds.; Plenum: New York, 1998.
(63) Adamo, C.; Barone, V. Toward Reliable Density Functional Methods Without Adjustable Parameters: The PBE0 Model. *J. Chem. Phys.* **1999**, *110*, 6158−6169.

(64) Ernzerhof, M.; Perdew, J. P. Generalized Gradient Approximation to the Angle- and System-Averaged Exchange Hole. *J. Chem. Phys.* **1998**, *109*, 3313−3320.
(65) Zhao, Y.; Truhlar, D. G. Comparative DFT Study of van der Waals Complexes: Rare-Gas Dimers Alkaline-Earth Dimers, Zinc Dimer, and Zinc-Rare Gas Dimers. *J. Phys. Chem.* **2006**, *110*, 5121−5129.
(66) Yanai, T.; Tew, D.; Handy, N. C. A New Hybrid-Exchange Correlation Functional Using the Coulomb-Attenuating Method. *Chem. Phys. Lett.* **2004**, *393*, 51−57.
(67) Chai, J.-D.; Head-Gordon, M. Systematic Optimization of Long-Range Corrected Hybrid Density Functionals. *J. Chem. Phys.* **2008**, *128*, 084106.
(68) MØller, C.; Plesset, M. S. A Note on an Approximation Treatment for Many-Electron Systems. *Phys. Rev.* **1934**, *46*, 0618−0622.
(69) Bartlett, R. J.; Purvis, G. D., III Many-Body Perturbation Theory, Coupled-Pair Many-Electron Theory, and Importance of Quadruple Excitations for Correlation Problem. *Int. J. Quantum Chem.* **1978**, *14*, 561−581.
(70) Pople, J. A.; Krishnan, R.; Schlegel, H. B.; Binkley, J. S. Electron Correlation Theories and Their Applications to the Study of Simple Reaction Potential Surfaces. *Int. J. Quantum Chem.* **1978**, *14*, 545−560.
(71) Pople, J. A.; Head-Gordon, M.; Raghavachari, K. Quadratic Configuration Interaction − A General Technique for Determining Electron Correlation Energies. *J. Chem. Phys.* **1987**, *87*, 5968−5975.
(72) Kobayashi, R.; Handy, N. C.; Amos, R. D.; Trucks, G. W.; Frisch, M. J.; Pople, J. A. Gradient Theory Applied to the Bueckner Doubles Method. *J. Chem. Phys.* **1991**, *95*, 6723−6733.
(73) Wilson, A. K.; Mourik, T. van; Dunning, T. H., Jr. Gaussian Basis Sets for Use in Correlated Molecular Calculations. VI. Sextuple Zeta Correlation Consistent Basis Sets for Boron Through Neon. *J. Mol. Struct.: THEOCHEM* **1996**, *388*, 339−349 and references therein.
(74) Merrick, J. P.; Moran, D.; Radom, L. An Evaluation of Harmonic Vibrational Frequency Scale Factors. *J. Phys. Chem. A* **2007**, *111*, 11683−11700.
(75) Andersson, M. P.; Uvdal, P. New Scale Factors for Harmonic Vibrational Frequencies Using the B3LYP Density Functional Method with the Triple-z Basis Set 6-311+G(d,p). *J. Phys. Chem. A* **2005**, *109*, 2937−2941.
(76) Gonzalez, C.; Schlegel, H. B. Reaction Path Following in Mass-Weighted Internal Coordinates. *J. Phys. Chem.* **1990**, *94*, 5523−5527.
(77) Reed, A. E.; Curtiss, L. A.; Weinhold, F. Intermolecular Interactions From a Natural Bond Orbital, Donor-Acceptor Viewpoint. *Chem. Rev.* **1988**, *88*, 899 and references therein.
(78) Karabulut, S.; Namli, H.: Leszczynski, J. Detection of Tautomer Proportions of Dimedone in Solution: A New Approach Based on Theoretical and FT-IR Viewpoint. *J. Comput.-Aided Mol. Des.* **2013**, DOI 10.1007/s10822-013-9669-z and references cited therein.
(79) Sigalov, M.; Shainyan, B.; Krief, P.; Ushakov, I.; Chipanina, N.; Oznobikhina, L. Intramolecular Interactions in Dimedone and Phenalen-1,3-dione Adducts 0f 2(4)-Pyridinecarboxaldehyde: Enol−Enol and Ring Chain Tautomerism. Strong Hydrogen Bonding, Zwitterions. *J. Mol. Struct.* **2011**, *1006*, 234−236.
(80) Bolte, M.; Scholtyssik, M. Dimedone at 133K. *Acta Crystallogr.* **1997**, DOI: 10.1107/S0108270197099423.
(81) Semmingsen, D. The Crystal and Molecular Structure of Dimedone. *Acta Chem. Scand.* **1974**, *28B*, 169−174.
(82) Singh, I.; Calvo, C. The Crystal Structure of Dimedone. *Can. J. Chem.* **1975**, *53*, 1046−1050.
(83) Cremlyn, R. J.; Osborne, A. G.; Warmsley, J. F. NMR Spectral Studies of Dimedone-Aldehyde Adducts Part 1. ^{1}H and ^{13}C NMR Spectral Studies of Dimedone. *Spectrochim. Acta, Part A* **1996**, *52*, 1423−1432.
(84) Alagona, G.; Ghio, C. Keto−Enol Tautomerism in Linear and Cyclic β-Diketones: A DFT Study in Vacuo and in Solution. *Int. J. Quantum Chem.* **2008**, *108*, 1840−1855.
(85) Dobrowolski, J. Cz.; Rode, J. E.; Sadlej, J. Cysteine Conformation Revisited. *J. Mol. Struct.: THEOCHEM* **2007**, *810*, 129−134.
(86) Sadlej, J.; Dobrowolski, J. C.; Rode, J. E.; Jamróz, M. H. Density Functional Theory Study on Vibrational Circular Dichroism as a Tool for Analysis of Intermolecular Systems: (1:1) Cysteine−Water Complex Conformations. *J. Phys. Chem. A* **2007**, *111*, 10703−10711.
(87) Wilke, J. J.; Lind, M. C.; Schaefer, H. F., III; Császár, A. G.; Allen, W. D. Conformers of Gaseous Cysteine. *J. Chem. Theory Comput.* **2009**, *5*, 1511−1523.
(88) Roux, M. V.; Foces-Foces, C.; Notario, R.; Ribeiro da Silva, M. A. V.; Ribeiro da Silva, M.; das, D. M. C.; Santos, A. F. I. O. M.; Juaristi, E. Experimental and Computational Study of Sulfur-Containing Amino Acids: L-Cysteine, L-Cystine, and L-Cysteine-Derived Radicals, S—S, S—H, and C—S Bond Dissociation Enthalpies. *J. Phys. Chem. B* **2010**, *114*, 10530−10540.
(89) Sanz, M. E.; Blanco, S.; López, J. C.; Alonso, J. L. Rotational Probes of Six Conformers of Neutral Cysteine. *Angew. Chem., Int. Ed.* **2008**, *47*, 6216−6220.
(90) Dobrowolski, J. C.; Jamróz, M. H.; Kolos, R.; Rode, J. E.; Sadlej, J. Theoretical Prediction and the First IR Matrix Observations of Several L-Cysteine Molecule Conformers. *ChemPhysChem* **2007**, *8*, 1085−1094.
(91) Gronert, S.; O'Hair, R. A. J. Ab Initio Studies of Amino Acid Conformations. 1. The Conformers of Alanine, Serine, and Cysteine. *J. Am. Chem. Soc.* **1995**, *117*, 2071.
(92) Chandra, S.; Saleem, H.; Sebastian, S.; Sundaraganesan, N. The Spectroscopic (FT-IR, FT-Raman), NCA, First-Order Hyperpolarizability, NBO Analysis, HOMO and LUMO Analysis of L-Cysteine by Ab Initio HF and Density Functional Method. *Spectrochim. Acta* **2011**, *78A*, 1515−1534.
(93) Fernández-Ramos, A.; Cabaleiro-Lago, E.; Hermida-Ramón, J. M.; Martınez-Nuñez, E.; A. Peña-Gallego, A. DFT Conformational Study of Cysteine in Gas Phase and Aqueous Solution. *J. Mol. Struct.: THEOCHEM* **2000**, *498*, 191−200.
(94) Pecul, M. Conformational Structures and Optical Rotation of Serine and Cysteine. *Chem. Phys. Lett.* **2006**, *418*, 1−10.
(95) Linder, R.; Seefeld, K.; Vavra, A.; Kleinermanns, K. Gas Phase Infrared Spectra of Nonaromatic Amino Acids. *Chem. Phys. Lett.* **2008**, *453*, 1−6.
(96) Riffet, V.; Frison, G.; Bouchoux, G. Acid-Base Thermochemistry of Gaseous Oxygen and Sulfur Substituted Amino Acids (Ser, Thr, Cys, Met). *Phys. Chem. Chem. Phys.* **2011**, *13*, 18561−18580.
(97) Schmidt, J.; Kass, S. R. Zwitterion vs Neutral Structures of Amino Acids Stabilized by a Negatively Charged Site: Infrared Photodissociation and Computations of Proline−Chloride Anion. *J. Phys. Chem. A* **2013**, *117*, 4863−4869 and references therein.
(98) de Grotthuss, C. J. T. Sur la Décomposition de l'eau et des Corps Qu'elle Tient en Dissolution à l'aide de l'électricité Galvanique. *Ann. Chim. (Paris)* **1806**, *58*, 54−73.
(99) Eigen, M. Proton Transfer, Acid-Base Catalysis, and Enzymatic Hydrolysis. Part 1: Elementary Processes. *Angew. Chem., Int. Ed. Engl.* **1964**, *3*, 1−19.
(100) Cukierman, S. Et tu Grotthuss. *Biochim. Biophys. Acta* **2006**, *1757*, 876−885.
(101) Markovitch, O.; Chen, H.; Izvekov, S.; Paesani, F.; Voth, A.; Agmon, N. Special Pair Dance and Partner Selection: Elementary Steps in Proton Transport in Liquid Water. *J. Phys. Chem. B* **2008**, *112*, 9456−9466 and references therein.
(102) Mai, B. K.; Park, K.; Duong, M. P. R. T.; Kim, Y. Proton Transfer Dependence on Hydrogen-Bonding of Solvent to the Water Wire: A Theoretical Study. *J. Phys. Chem. B* **2013**, *117*, 307−315.